Journal of Thermal Analysis and Calorimetry, Vol. 78 (2004) 885–895

NON-ISOTHERMAL CRYSTALLIZATION OF POLYETHYLENES AS FUNCTION OF COOLING RATE AND CONCENTRATION OF SHORT CHAIN BRANCHES

I.S. Kolesov[*], *R. Androsch and H.-J. Radusch*

Martin Luther University Halle-Wittenberg, Institute of Materials Science, D-06099 Halle, Germany

Abstract

Non-isothermal crystallization and melting of metallocene-catalyzed polyethylene was analyzed using the power-compensating calorimetry as function of both cooling rate and branch-degree ranging from 1 to 300 K min^{-1}, and from 0 to 72 hexyl-branches per 1000 carbon atoms, respectively. The onset crystallization temperature decreases linearly with increasing logarithm of cooling rate. The slope of this dependence increases with increasing branch-degree, which is explained by a stronger inhibition of the crystallization by the branches and the decreasing diffusion rate of molecules. The melting endotherms reveal a clear reduction of the crystallinity in the entire temperature range with increasing cooling rate.

Keywords: high-speed differential scanning calorimetry, melting, non-isothermal melt-crystallization, poly(ethylene-*co*-1-octene)

Introduction

The crystallization and melting behavior of homogeneous ethylene-1-alkene-copolymers synthesized with single-site-catalysts was extensively investigated in last decade [1–7]. During the non-isothermal crystallization of ethylene-1-alkene-copolymers the concentration of the short chain branches (SCB) appears as further decisive parameter additionally to the rate of cooling from the melt. Increasing SCB-concentration entails the reduction of the length of crystallizable ethylene sequences. The total crystallinity, the perfection and the size distribution of the crystals are controlled by the SCB-concentration as well as by the cooling rate [1–7]. Recent investigations on polyethylene and ethylene copolymers by means of differential scanning calorimetry (DSC) were accomplished at cooling rates no larger than 40 K min^{-1} [1 – 5, 7]. Non-isothermal crystallization of poly(ethylene-*co*-1-octene) at rapid cooling rates of some thousands K min^{-1} was investigated using the thermal-optical method of Ding-Spruiell [6]. It was assumed that rapid cooling [6] as well as high

---

[*] Author for correspondence: E-mail:igor.kolesov@iw.uni-halle.de

1388–6150/2004/ $ 20.00

Akadémiai Kiadó, Budapest
Kluwer Academic Publishers, Dordrecht

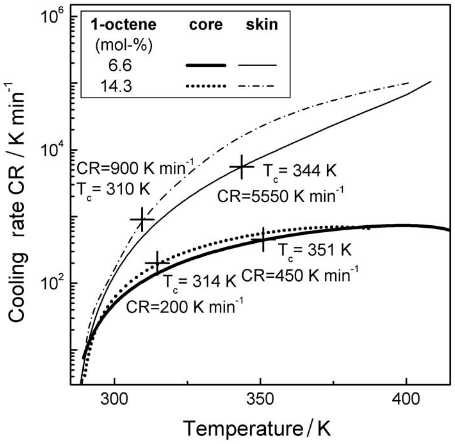

Fig. 1 Calculated dependence of the cooling rate on the temperature of injection-molded poly(ethylene-*co*-1-octene) plates with a thickness of 1 mm during solidification with the melt temperature and the initial temperature of the mold of 288 and 423 K, respectively

SCB-concentration [4, 7], *i.e.* high undercooling, lead to an increased incorporation of SCBs into the crystals, which is not unequivocally discussed in the literature [5].

At the most common processing methods crystallization of polymers occurs at enormously high cooling rates. The dependencies of the effective cooling rate on temperature of poly(ethylene-*co*-1-octene) injected into quadrat-shaped mold cavity with a gap of 1 mm during the solidification of melt were modeled using the 'MoldFlow' software and are shown in Fig. 1. Required physical constants such as thermal conductivity or density for the materials under study were taken from the data bank of the software. The simulation was performed based on the assumption that the mold-temperature is constant and uniformly distributed. The calculated time-dependent temperature profiles were later transformed to the dependencies of the effective cooling rate on melt temperature. The crosses in Fig. 1 mirror the values of crystallization onset-temperature and corresponding effective cooling rate chosen in agreement with experimental data which are described beneath in present work (see Fig. 4). From the Fig. 1 can be concluded that in the core of the plates the effective cooling rate in the temperature range of the non-isothermal primary crystallization does not exceed 500 K min^{-1}. At the same time the cooling rate achieves about 5000 K min^{-1} in the skin layer.

By Mathot and coworkers [8] it was experimentally proven that the experiments at the practice-relevant heating and cooling rates of some hundreds K min^{-1} are technically realizable in a power-compensating differential scanning calorimeter.

In connection with the above presented facts the goal of the present work is to perform a systematic study of the influence of cooling rate on the non-isothermal crystallization and the subsequent melting behavior of poly(ethylene-*co*-1-octene)s in a broad range of cooling rates and SCB contents.

Experimental

Materials

The materials used in this study are the metallocene-catalyzed homogeneous poly(ethylene-*co*-1-octene) random copolymers. The poly(ethylene-*co*-1-octene)s are commercial products of DuPont Dow Elastomers. Linear polyethylene, having high density was used as reference object. Details about the synthesis and the structure of the linear polyethylene are given elsewhere [9]. Films of 50 – 250 μm thickness were prepared by compression-molding, using a cooling rate of 1 K min^{-1} or by quenching in cold water. Subsequently, the films were stored at room temperature before analysis. The molecular characteristics of all materials under study are shown in Table 1. Table 1 includes additionally the densities at a temperature of 296 K as function of the crystallization history. Flat specimens in disc shape with a diameter of 5 mm were punched from these films for DSC analysis.

Table 1 Molecular characteristics of used poly(ethylene-*co*-1-octene), effect of thermal history on the density

1-octene content[1]/ mol %	Short-chain branches per 1000 C (average)	Molecular mass /kg mol^{-1}			Polydispersity M_w/M_n	Density [2] kg m^{-3}
		M_n	M_w	M_z		
0.0	0.0	102.0	357.0	–	3.5	954(sc) 939(q)
4.6	23.0	27.0	48.6	79.5	1.8	914(sc) 905(q)
6.6	33.0	31.0	53.4	89.7	1.7	904(sc) 901(q)
10.1	50.5	33.9	61.1	105.2	1.8	883(sc) 883(q)
14.3	71.5	39.0	70.5	122.9	1.8	874(sc) 876(q)

[1] according to manufacturer information

[2] by density-gradient column, obtained on slowly cooled (sc) at –1 K min^{-1} and quenched (q) samples

Instrumentation

The investigations at heating and cooling rates from 1 to 300 K min^{-1} were performed using a power-compensating differential scanning calorimeter DSC 7 (Perkin-Elmer) equipped with the liquid nitrogen accessory CCA-7 for controlled cooling and with the *PYRIS* software for controlling and evaluation of the measurements. In order to achieve a fast heat transfer between heater/sensor and sample and as well as a linear relationship between the sample temperature and time, we used helium as purge gas at a flow rate of 50 mL min^{-1}, a relatively low sample mass of about 1 mg and a low heat-sink temperature of 123 K. Samples were sealed in small 10 μL aluminum pans.

The sample-furnace temperature was calibrated by the onset-temperatures of melting of indium, tin, zinc, and cyclopentane as well as solid-solid phase transition of adamantane on heating at a rate of 10 K min^{-1} [10]. The initial heat-flow rate calibration was done using the heat of fusion of indium. The heat-flow-rate raw data were corrected for the instrumental asymmetry, and converted into apparent-heat-capacity data, using sapphire as standard [11]. The measured apparent heat capacity in conjunction with theoretical values of heat capacity for crystalline and amorphous polyethylene, taken from the *A*dvanced *TH*ermal *A*nalysis *S*ystem (ATHAS) [12] were utilized for calculation of an enthalpy-based crystallinity on the basis of the two-phase model as described in [1].

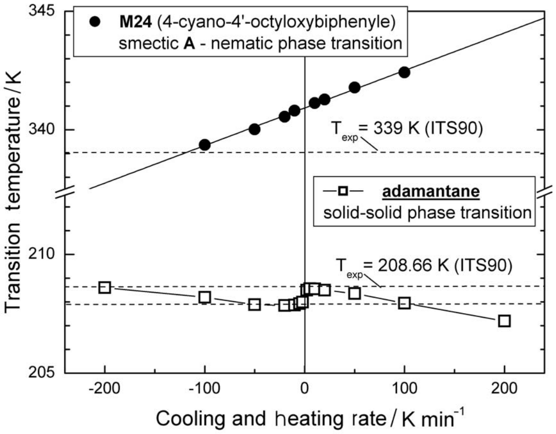

Fig. 2 Measured values of the transition temperature for the adamantane and the 4-cyano-4'-octyloxybiphenyl (M24) *vs*. the cooling/heating rate with the expected transition temperature values

An additional correction of the instrumental data of crystallization and melting temperatures was performed using the smectic **A** – nematic phase second order transition of the liquid crystal M24 (4-cyano-4′-octyloxybiphenyle) [8, 10, 11, 13] in a wide range of heating and cooling rates. Figure 2 shows the transition temperatures together with the solid-solid phase first order transition of adamantane recorded as a function of the cooling and heating rate. For comparison, the expected temperatures of the mentioned transition are also given in Fig. 2. The adamantane which was used for temperature calibration exhibits only a weak change of the transition onset-temperature as a function of the cooling and heating rate, and excellent agreement with the ITS90 value. The analysis of the smectic **A** – nematic phase second order transition of the liquid crystal M24 for calibration of the temperature is difficult due to the non-explained appearance as peak in connection with the low signal-to-noise ratio. The peak temperature changes linearly by more than 2 K when the rate of temperature change is increased to 200 K min^{-1}.

Results

Effect of cooling rate and SCB content on the melt-crystallization

The temperature dependencies of the apparent specific heat capacity, c_p, and of the crystallinity, calculated on this basis are shown in Fig. 3 a and b, respectively, for the sample with 14.3 mol% of 1-octene as example. The data reveal a marked decrease of the primary crystallization temperature of poly(ethylene-*co*-1-octene) with increasing rate of cooling from the melt. Some increase of temperature hysteresis between melting and crystallization regions with increasing cooling rate should be also noted. As Fig. 4 illustrates, the experimentally determined dependence of the corrected onset-temperature of non-isothermal crystallization $T_{\mathrm{c,onset}}$ *vs.* the logarithm

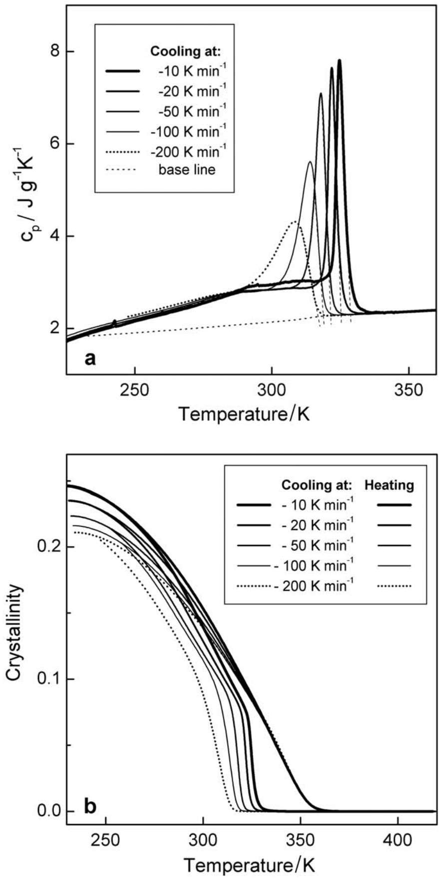

Fig. 3 Apparent specific heat capacity c_p (a) and enthalpy-based crystallinity (b) of poly(ethylene-*co*-1-octene) with 14.3 mol% of 1-octene *vs*. temperature measured during cooling from the melt at several rates and during subsequent heating at 100 K min^{-1}

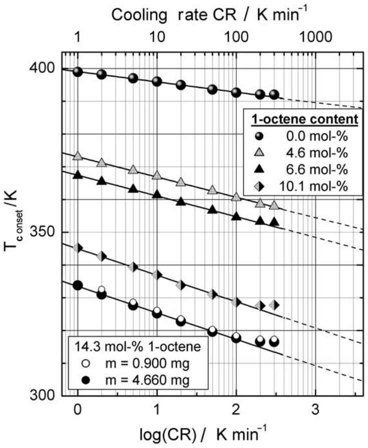

Fig. 4 Effect of 1-octene content on the onset temperature of non-isothermal crystallization of poly(ethylene-*co*-1-octene) *vs*. cooling rate. The bottom plot shows also an influence of sample mass (m)

of the cooling rate log(CR) can be good approximated by linear regression in a broad range of cooling rates. Thus, the crystallization temperature $T_{c,onset}$ *vs.* cooling rate CR is formally described by the equation $T_{c,onset} = a - b \log(CR)$, where *a* and *b* are constants. It is quite obvious that an increase of the 1-octene content, in addition to the drastic decrease of the crystallization temperature within the entire range of the cooling rates, causes also a significant increase of the slope of $T_{c,onset}$ *vs.* log(CR) function. Thus, the coefficient *b* increases from the value of 3.14, determined for linear polyethylene, to 6.17 and 8.08 for the poly(ethylene-*co*-1-octene)s with a 1-octene content of 4.6 and 14.3 mol%, respectively. These dependencies of $T_{c,onset}$ *vs.* log(CR) (Fig. 4) for poly(ethylene-*co*-1-octene) with a 1-octene content of 14.3 mol% demonstrate that a significant increase of the sample mass causes only a slight decrease of $T_{c,onset}$, by about 1 K in the entire cooling rate range. This behavior is additional evidence of an only slight effect of the thermal lag on the determined onset-values of transition temperatures.

Effect of thermal history and SCB content on the melting behavior

While for linear polyethylene both, the temperature of the melting peak and the crystallinity in the entire temperature range decrease as expected with increasing cooling rate in the preceding non-isothermal melt-crystallization (Figs 5 a and b), the melting behavior of branched polyethylenes is substantially more complicated. Despite the high heating rate of 100 K min^{-1} generally used for all branched polyethylenes, a recrystallization was observed. Multiple melting behavior becomes more pronounced with decreased heating rate (compare Figs 5 c and d) and especially with increasing branch degree of polyethylene (compare Figs 5 c and e/f). In this connection the influence of the thermal history on the melting behavior of short chain

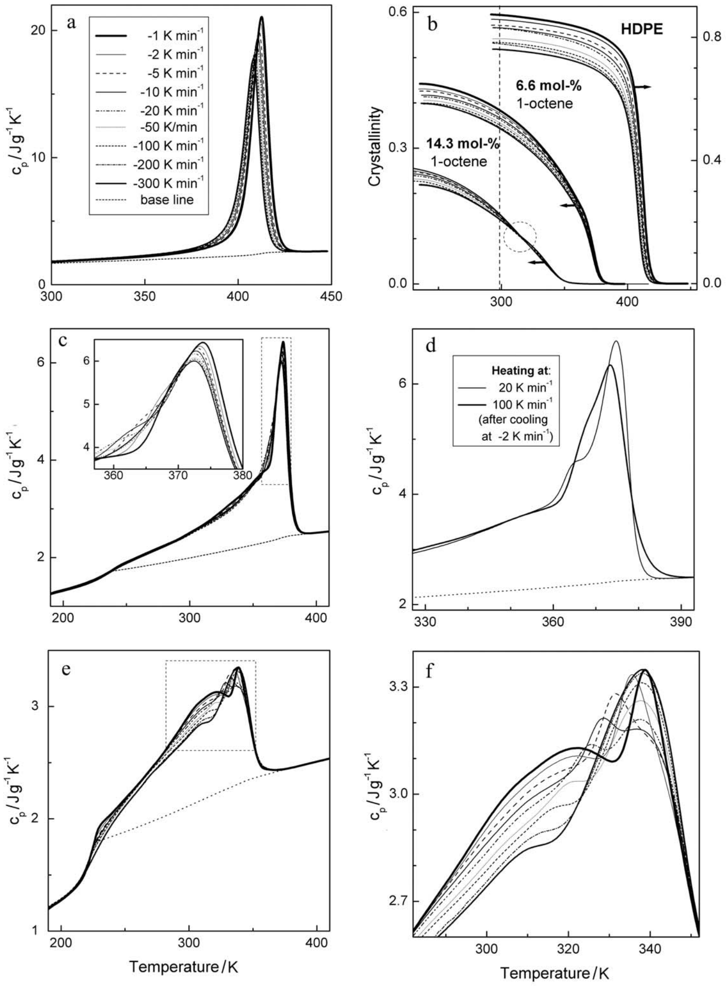

Fig. 5 Apparent specific heat capacity c_p (a, c - f) and enthalpy-based crystallinity (b) of poly(ethylene-*co*-1-octene) with 1-octene content of 0.0 (a), 6.6 (c, d) and 14.3 mol% (e, f) *vs*. temperature measured during heating at 100 K min^{-1} immediately after cooling from the melt at several rates. Fig. 5f and insert in Fig. 5c show the enlargement of the marked area in Fig. 5e and 5c, respectively

branched polyethylene is discussed below more detailed for poly(ethylene-*co*-1-octene) with high 1-octene content as example.

At low cooling rates of 1 or 2 K min^{-1} the melting endotherms of poly(ethylene-*co*-1-octene) with an 1-octene content of 14.3 mol% (Figs 5 e and f) exhibit a relatively narrow and intense peak at a temperature of approximately 339 K and one diffuse broad peak at about 322 K with a shoulder between 300 and 310 K. The maximum-temperature and height of the latter peaks decrease with increasing cooling

Table 2 Effect of cooling rate and comonomer content on the melting temperature and enthalpy-based crystallinity of poly(ethylene-*co*-1-octene) with 1-octene content of 0.0, 6.6 and 14.3 mol%

Cooling rate from the melt/ K min^{-1}	Crystallinity/%[1]			Melting temperature/K[2]		
	0.0 mol%	6.6 mol%	14.3 mol%	0.0 mol%	6.6 mol%	14.3[3] mol%
1	87.3	38.5	15.6	412.5	373.8	338.7
2	85.8	37.8	15.4	411.9	373.4	–
5	84.0	37.4	15.3	411.2	373.0	–
10	83.1	36.8	15.0	410.6	372.7	337.3
20	82.3	36.4	14.9	410.0	372.5	337.5
50	79.5	35.7	14.6	409.3	372.5	337.7
100	78.3	35.2	14.3	408.8	372.5	338.0
200	77.6	34.7	14.5	408.3	372.5	338.2
300	76.1	34.5	14.4	408.1	372.5	338.2

[1] calculated at 298 K from heating scans
[2] peak-temperature in the DSC melting endotherm
[3] final remelting peak

rate. At cooling rates of between 100 and 300 K min^{-1} the previously more intense peak degenerates into a weak shoulder. At cooling rates of between 10 and 20 K min^{-1} a new and considerably broader peak develops and grows rapidly with increasing rate of cooling from the melt replacing a narrow intensive peak. Figures 5 e and f demonstrate well also the decrease of the apparent heat capacity with decreasing rate of cooling from the melt in the entire temperature range from the glass transition to the melting peaks.

It should be noted that the melting behavior of poly(ethylene-*co*-1-octene)s with a medium 1-octene content is partly similar to that described above. However, it is observed in a more narrow temperature range. All heating scans recorded after cooling from the melt at different rates of ≥ 10 K min^{-1} exhibit final remelting peaks close to virtually equal temperatures (see the insert in Fig. 5 c, Fig. 5 f and Table 2).

The enthalpy-based crystallinity of all poly(ethylene-*co*-1-octene)s measured subsequent to the non-isothermal melt-crystallization, decreases as expected with increasingly rate of cooling from the melt and with increasing SCB-concentration (Fig. 5 b). However, an absolute and relative change in the crystallinity, determined at an identical temperature, decreases as result of increasing cooling rate more distinct with increasing SCB-concentration (see Table 2). For example, an absolute change in the crystallinity at 298 K with increasingl cooling rate from 1 to 300 K min^{-1}($\Delta\chi'_{1\div 300\ \mathrm{K/min}}$) amounts to 11.2, 4.0 and 1.2% for poly(ethylene-*co*-1-octene) with 1-octene content of 0.0, 6.6 and 14.3 mol%, respectively. At the same time a relative change in the crystallinity ($\Delta\chi'_{1\div 300\mathrm{K/min}}/\chi'_{10\mathrm{K/min}}$)·100 % amounts to 13.5, 10.9 and 8.0%, respectively. The above described behavior occurs in the entire temperature range for linear polyethylene and for copolymers with medium content of 1-octene. However, the curves of crystallinity *vs.* temperature of copolymers with high 1-octene content exhibit one region of cross-over close to the first peak or shoulder of melting endotherms (*i.e.*, 310 – 330 K for 14.3 mol% of 1-octene).

Discussion and conclusions

Effect of cooling rate and SCB content on the melt-crystallization

First of all, it should be noted that the experimentally observed decrease of the onset-temperature of non-isothermal melt-crystallization $T_{c,onset}$ with increasing cooling rate is not associated with the thermal lag of the calorimeter. Important evidence for this conclusion is an only slight change of the crystallization onset-temperature by less than 1 K with increasing rate of temperature change from 1 to 200 K min^{-1}, measured on adamantane used by basic calibration of instrument. The lowering of $T_{c,onset}$ with increasing cooling rate is also indirectly proven by the changes of the subsequent melting behavior as a function of cooling rate during melt-crystallization, which is discussed below. At the same time it should be noted that the values of peak temperatures and the shape of entire peak (Fig. 3) are certainly affected by thermal lag.

The drop of the temperature of primary non-isothermal crystallization with increase of both, SCB-concentration, and rate of cooling from the melt is explained by growing kinetic constraints for the process of diffusion of crystallizable ethylene sequences to the crystal growth front. The increase of SCB-concentration results in a general increase of the supercooling required for crystallization, which is a well-established experimental and theoretically explained fact for poly(ethylene-*co*-1-octene)s [1–7]. Thus, in addition to the sterical hindrances of the crystallization caused by SCBs the crystallization rate is controlled by the low rate of diffusion of the molecular chains as a result of an overall decrease in crystallization temperature. For these two reasons the lowering of $T_{c,onset}$ with increasing rate of cooling from the melt becomes more radical with growing SCB-concentration.

The empirically acquired linear relationship between the onset temperature of non-isothermal crystallization and the logarithm of cooling rate is of interest to theory and practice. This relationship can be used to estimate the crystallization temperature at cooling rates which are typical for the skin layer of specimens in polymer processing e.g. by means of injection molding or extrusion. Additionally the theoretical analysis of the relation between the onset-temperature of non-isothermal crystallization and the cooling rate would permit to interpret the information supplied by the slope of this relationship as well as the estimation of the validity range for the empirically determined mathematical relation ($T_{c,onset} = a - b \cdot \log(\mathrm{CR})$). In this context a certain deviation of experimental points from the straight line at the values of cooling rate of more than 100 K min^{-1} should be noted (Fig. 4). The results of this work demonstrate also that with the use of helium purge in power-compensating differential scanning calorimeter DSC-7 a successful simulation of the temperature conditions of crystallization in the core of injection molded or extruded specimens is possible.

Effect of thermal history and SCB content on the melting behavior

The peculiarities of the melting behavior of non-isothermal melt-crystallized poly(ethylene-*co*-1-octene)s compared to linear polyethylene is caused by the existence of low-stable populations of orthorhombic lamellar crystals and a pseudo-hexagonal mesophase [4–6].

Sufficiently slow cooling from the melt (e.g. at 1 K min^{-1}) results in formation of population of relatively perfect and stable orthorhombic crystals, the melting of which gives a narrow high-temperature peak. With increasing cooling rate and SCB-concentration the temperature of primary crystallization and crystal size decrease, and the concentration of defects in the crystals becomes higher. That explains the shift of the discussed peak towards lower temperatures and its degeneration to a shoulder at high cooling rates. As already mentioned earlier [4] a certain part of the macromolecules of poly(ethylene-*co*-1-octene)s preserves the capability for crystallization up to the glass transition temperature. The reduction of the temperature of primary crystallization with growing SCB-concentration and rate of cooling from the melt result in a reduction of stability and melting point of the crystals.

Recent investigation by means of temperature-resolved derivative FTIR [14] revealed that in poly(ethylene-*co*-1-octene)s non-equilibrium pseudo-hexagonal mesophase appears and grows in volume for higher SCB-concentration and with increasing rate of cooling from the melt. During heating this mesophase almost completely disappears near 325 K [14]. Different populations of low-stable orthorhombic crystals melt also in a broad temperature range between the glass transition temperature and the temperature of primary non-isothermal crystallization, e.g. 310 - 330 K for poly(ethylene-*co*-1-octene) with 1-octene content of 14.3 mol% depending on the cooling rate. Subsequent recrystallization occurs in presence of a population of more stable orthorhombic crystals which now play a role of nuclei [7]. The self-seeding effect of the most stable crystal population [7] is responsible for the fact that all heating scans recorded after cooling from the melt at different rates ≥ 10 K min^{-1} exhibit final remelting peaks close to equal temperatures (see Table 2). It should be also noted that self-seeding in short-chain-branched polyethylenes has a distinct effect in a broad temperature range. This is the basis for successful investigation of such polyethylenes by means of successive self-nucleation/annealing method (see for example [15]).

The decrease of the apparent heat capacity with increasing rate of cooling from the melt, observed in the entire temperature range, can be explained by formation of mesophase and/or larger number of considerably smaller and disordered orthorhombic crystals which both are characterized by a lower specific enthalpy of fusion.

The cross-over of the temperature-dependent crystallinity, i.e., the fact that at high temperature quickly cooled samples exhibit a higher crystallinity than slowly cooled samples, is obtained only on copolymers with 14.3 mol% 1-octene, and must be connected with the above discussed recrystallization. A similar cross-over phenomenon was observed by Goderis *et al*. [16] for poly(ethylene-*co*-1-octene)s with medium 1-octene content of 5.5 mol%. The quenched preparation, unexpectedly, revealed a higher crystallinity than the corresponding slowly cooled sample, which was explained by more pronounced ‘co-recrystallization’ involving ‘non-ordered ethylene sequences’. The latter data, however, were collected after the samples reached metastable equilibrium, and can therefore not be compared with our results.

* * *

The authors gratefully acknowledge financial support by Deutsche Forschungsgemeinschaft (DFG). Samples of polyethylenes were kindly provided by Omya GmbH (Germany), or tailor-synthesized by Dr. S. Rudolph (Martin Luther University Halle-Wittenberg, Germany). Samples of adamantane and of liquid crystal M24 (4-cyano-4′-octyloxybiphenyl) were kindly provided by Dr. S. Neuenfeld (Merck KGaA, Germany). Thanks are due to Dr. C. Gabriel (Friedrich Alexander University Erlangen-Nürnberg) for the molecular characterization of poly(ethylene-*co*-1-octene)s.

References

1 V. B. F. Mathot, R. L. Scherrenberg, M. F. J. Pijpers and W. Bras, J. Therm. Anal., 46 (1996) 681.
2 V. B. F. Mathot, R. L. Scherrenberg and M. F. J. Pijpers, Polymer, 39 (1998) 4541.
3 Man-Ho Kim and P. J. Phillips, J. Appl. Polym. Sci., 70 (1998) 1893.
4 R. Androsch, Polymer, 40 (1999) 2805.
5 A. Alizadeh, I. Richardson, J. Xu, S. McCartney, H. Marand, Y. W. Cheung and S. Chum, Macromolecules, 32 (1999) 6221.
6 J. Wagner, S. Abu-Iqyas, K. Monar and P. J. Phillips, Polymer, 40 (1999) 4717.
7 R. Androsch and B. Wunderlich, Macromolecules, 33 (2000) 9076.
8 T. F. J. Pijpers, V. B. F. Mathot, B. Goderis, R. L. Scherrenberg and E. W. van der Vegte, Macromolecules, 35 (2000) 3601.
9 S. Rudolph, J. Giesemann, J. Kressler, T. J. Menke, H. Menge and P. Arends, J. Appl. Polym. Sci., 74 (1999) 439.
10 S. M. Sarge, G. W. H. Höhne, H. K. Cammenga, W. Eysel and E. Gmelin, Thermochim. Acta, 361 (2000) 1.
11 B. Wunderlich, Thermal Analysis; Academic Press, Boston 1990.
12 Advanced THermal Analysis System: B. Wunderlich, Pure Appl. Chem., 67 (1995) 1919. For downloadable data use WWW (Internet): URL: http//web.utk.edu/~athas.
13 G. W. H. Höhne, J. Schawe and C. Schick, Thermochim. Acta, 221 (1993) 129.
14 R. Androsch, I. Kolesov and H.-J. Radusch, J. Therm. Anal. Cal., 73 (2003) 59.
15 K. Czaja, B. Sacher and M. Bialek, J. Therm. Anal. Cal., 67 (2002) 547.
16 B. Goderis, M. Peeters, V. B. F. Mathot, M. H. J. Koch, W. Bras, A. J. Ryan and H. Reynaers, J. Polym. Sci., Part B: Polym. Phys., 38 (2000) 1975.